Original Article

Three-dimensional magnetic resonance neurography aids in detection of brachial plexus nerve root signal and size alterations in patients with amyotrophic lateral sclerosis: a case-control study

Shanshan Wang[1,2], Xiao Man[3], Yufan Chen[1], Tao Gong[2], Fei Gao[2], Weibo Chen[4], Guangbin Wang[2], Bin Zhao[2], Avneesh Chhabra[5]

[1]Department of Radiology, Shandong Provincial Hospital, Shandong University, Jinan, China; [2]Department of Radiology, Shandong Provincial Hospital Affiliated to Shandong First Medical University, Jinan, China; [3]Department of Neurology, Shandong Provincial Hospital Affiliated to Shandong First Medical University, Jinan, China; [4]Philips Healthcare, Shanghai, China; [5]Department of Radiology, UT Southwestern Medical Center, Dallas, TX, USA

Contributions: (I) Conception and design: S Wang, Y Chen, G Wang, A Chhabra; (II) Administrative support: T Gong, G Wang, B Zhao; (III) Provision of study materials or patients: S Wang, X Man; (IV) Collection and assembly of data: S Wang, Y Chen, W Chen; (V) Data analysis and interpretation: S Wang, X Man, Y Chen, T Gong, F Gao; (VI) Manuscript writing: All authors; (VII) Final approval of manuscript: All authors.

Correspondence to: Guangbin Wang, MD, PhD. Department of Radiology, Shandong Provincial Hospital Affiliated to Shandong First Medical University, 324 Jingwu Road, Jinan 250021, China. Email: wgb7932596@hotmail.com.

Background: Since previous histopathological studies have shown a distal to proximal gradient of axonal damage in peripheral nerves of patients with amyotrophic lateral sclerosis (ALS), it would be worthwhile to evaluate consequence of such changes on magnetic resonance imaging (MRI). The aim of this study was to assess proximal-distal longitudinal signal and size alterations of brachial plexus nerve roots in ALS patients using 3-dimensional (3D) magnetic resonance neurography (MRN).

Methods: A total of 21 ALS patients and 19 controls were evaluated. The diameters and signal-to-noise (SNR) ratio values of C5–C8 roots were measured at five points from proximal to distal sites. Student's *t*-test was performed to compare the differences at each point between two groups. Linear regression was performed for each nerve root, and the differences in linear regression slopes between two groups were analyzed. Receiver operating characteristic (ROC) analysis was performed for the diameter and SNR value ratio of the distal to the proximal points.

Results: Interobserver agreement was excellent [intraclass correlation coefficient (ICC): 0.802–0.913]. The diameters and SNR values of C5–C8 roots showed a significant decrease ($P<0.05$) from proximal to distal except SNR value of C5 root in controls. The slope values of diameters in ALS were −0.01924 for C5, −0.04404 for C6, −0.06228 for C7, and −0.06464 for C8. The slope values of SNR values in ALS were −10.14 for C5, −12.86 for C6, −15.99 for C7, and −19.06 for C8. The slope of nerve diameters and SNR values for ALS patients were more negatively sloped than controls ($P<0.05$) except SNR values of C5 and C7 roots. The ROC analysis confirmed that the diameter and SNR value ratio could differentiate ALS patients from controls with high accuracy. The cutoff values of diameter ratio were 0.7418 for C5, 0.6952 for C6, 0.6431 for C7, and 0.7147 for C8. The cutoff values of SNR value ratio were 0.5989 for C5, 0.6516 for C6, 0.6065 for C7, and 0.6758 for C8.

Conclusions: Proximal-distal longitudinal diameters and SNR values decreased significantly for brachial plexus nerve roots in ALS patients with larger differences in slopes compared to controls. These results reflect pathophysiological changes of ALS and may be helpful in improving the diagnosis of ALS.

Keywords: Amyotrophic lateral sclerosis (ALS); magnetic resonance imaging (MRI); magnetic resonance neurography (MRN); 3-dimensional (3D); brachial plexus

Submitted Jun 09, 2023. Accepted for publication Sep 21, 2023. Published online Oct 27, 2023.
doi: 10.21037/qims-23-833
View this article at: https://dx.doi.org/10.21037/qims-23-833

Introduction

Amyotrophic lateral sclerosis (ALS) is a fatal neurodegenerative disorder characterized by upper and lower motor neuron loss of the human nervous system, leading to progressive weakness of the bulbar, limb, thoracic, and abdominal muscles (1). Progressive motor neuron degeneration is the most predominant neurophysiologic change of ALS (2). Growing evidence indicates that the peripheral nervous system is affected in ALS pathogenetic cascade, especially at an early stage, including axonal degeneration, neuroinflammation, and Wallerian degeneration of fibers (3). Increasing evidence indicates that ALS is a distal axonopathy, with a distal to proximal gradient of damage in peripheral nervous system (4).

Detecting imaging abnormality of peripheral nerves may help to assess pathophysiological changes of ALS and to eventually improve diagnosis in ALS. Magnetic resonance neurography (MRN) has been widely used in the assessment of peripheral neuropathy (5-7), providing structural information to complement the functional information of neurophysiologic tests. There is limited literature on using MRN for ALS with heterogeneous results (8,9). Although Staff *et al.* qualitatively showed ALS lesions of the brachial plexus, which appeared similar to multifocal motor neuropathy lesions, no quantitative measurements were obtained in their work (10). They also did not use 3-dimensional (3D) MRN and it is common for the peripheral nerves and unsuppressed adjoining veins to exhibit isointense signal alterations on 2-dimensional (2D) short tau inversion recovery and T2-weighted images (T2WI) limiting the assessment of abnormal signal alterations of the obliquely coursing nerves of the plexi.

3D nerve-sheath signal increased with inked rest-tissue rapid acquisition of relaxation imaging (3D SHINKEI) is an MRN sequence that includes a combination of two preparation pulses and 3D turbo spin-echo sequence with T2-weighting. It enables vascular signal suppression and superior 3D visualization of detailed anatomy of the brachial plexus in high spatial resolution (11,12). However, patients with ALS have not been assessed quantitatively on imaging or using 3D SHINKEI.

Since previous histopathological studies have shown a distal to proximal gradient of axonal damage in peripheral nerves of patients with ALS (4), it would be worthwhile to evaluate consequence of such changes on magnetic resonance imaging (MRI). The aim of this study was to assess the proximal-distal longitudinal signal and size alterations of the brachial plexus roots using nerve-selective sequence, 3D SHINKEI. We present this article in accordance with the MDAR reporting checklist (available at https://qims.amegroups.com/article/view/10.21037/qims-23-833/rc).

Methods

Study participants

The study was conducted in accordance with the Declaration of Helsinki (as revised in 2013). The study was approved by the institutional ethics committee of Shandong Provincial Hospital and informed consent was provided by all individual participants. A total of 22 patients with sporadic ALS and 19 healthy controls (HCs) were recruited consecutively from December 2017 to July 2019 at Shandong Provincial Hospital. All participants with ALS had received a neurologic and electrophysiological examination by a neurologist specializing in peripheral nerve disorders with 23 years of experience in neurology. The inclusion criterion was a diagnosis of ALS in adult patients of all genders [clinically definite or probable by El Escorial criteria (13)]. All patients with ALS had clinical signs of lower motor neuron involvement (i.e., weakness, atrophy and/or fasciculations) in the forearm or hand. HC cases with no history of neurologic, psychiatric, or other major medical illnesses were recruited from friendship groups of patients with ALS and by word of mouth and were matched with regard to age.

MRN protocol

The scans were acquired on a 3 Tesla MR system (Ingenia, Philips Healthcare, Best, Netherlands) with a 16-channel neurovascular coil. Bilateral imaging of the brachial plexus was performed using 3D SHINKEI. The remaining protocol was used to exclude other diseases, including

coronal T1-weighted spin-echo images [time to repeat (TR) 564 ms; time to echo (TE), 7.3 ms; flip angle, 90°; number of signal averages (NSA), 2; slice thickness, 3 mm; gap, 0.3 mm], fat-suppressed coronal short tau inversion recovery images [TR, 2,826 ms; TE, 90 ms; inversion time (TI), 160 ms; flip angle, 90°; NSA,1; slice thickness, 3 mm; gap, 0.3 mm]. 3D SHINKEI was performed with the following parameters: TR, 2,200 ms; TE, 90 ms; TI, 250 ms, field of view (FOV) = 280 mm × 400 mm, echo-train length (ETL) =100, matrix =232×321, the reconstructed voxel size =0.45×0.45×1.0 mm^3, improved motion-sensitized driven equilibrium (iMSDE) duration =35 ms, phase encoding direction; right to left, percentage of phase oversampling =50%, acquisition time =6 min 06 s.

Data processing

Nerve root assessment of ALS patients and HCs was performed on 3D SHINKEI by two experienced neuroradiologists (SW and GW with 20 and 5 years of experience in neuroradiology, respectively) who were blinded to the diagnosis and electrophysiological examination findings. The nerve root segment was defined from a level immediately inferior to the spinal ganglia to the level of junction of brachial plexus root and trunk. The lengths of C5–C8 nerve root segments were standardized respectively using the mean length of all participants' roots as a standard. On this basis, the slope values of diameter and signal-to-noise (SNR) ratio value in C5–C8 roots were measured respectively. For each of the C5–C8 nerve roots, curved surface reconstruction of the whole root was performed and then divided into 5 equal segments. Regions of interest (ROIs) were placed in the center of each segment on the axial reformatted images that were perpendicular to the course of each root (in turn, named 1 through 5 from proximal to distal points), as illustrated in *Figure 1*. The diameter was calculated by the mean of longest diameter and shortest diameter at each point. The SNR was calculated as follows: SNR = SI (root)/SD (noise), where SI (root) is the signal intensity of the roots of brachial plexus, and SD (noise) is the standard deviation of the background noise measured in an ROI drawn outside of the image.

Statistical analyses

Statistical analysis was performed using the software GraphPad Prism Version 8 (GraphPad Software, San Diego, CA, USA). Chi-square test was used to determine differences in gender between ALS patients and HCs. Student's *t*-test was used to determine differences in age, height, and weight between ALS patients and HCs and differences between left and right sides. The inter-observer agreement of the diameters and SNR values was assessed using intraclass correlation coefficient (ICC) analysis. The ICC ranges of reliability values provided by Landis and Koch were used as the reference standard (14).

The average data from both observers was used to calculate the case-control differences. Student's *t*-test was performed to compare the differences at each point of C5–C8 nerve roots between ALS patients and HCs. Linear regression was performed for the diameters and SNR values of each root, and the differences in linear regression slopes between the two groups were analyzed by chi-square test. Receiver operating characteristic (ROC) curve analysis was obtained to evaluate the diagnostic performance of the diameter ratio and the SNR value ratio of the distal point (point 5) to the proximal point (point 1) in C5–C8 roots. The area under the ROC curve (AUC), cut-off values, sensitivity, and specificity were calculated. Statistical significance was denoted by $P<0.05$.

Results

Finally, 19 HCs and 21 patients with ALS were included as one patient was excluded due to the unclear nerve roots from chronic diffuse atrophy on 3D SHINKEI limiting the nerve root assessment. There were no significant differences in age, sex, weight, or height between the two groups. *Table 1* shows the demographics of the ALS patients and HCs.

ICCs for inter-observer agreement of diameter measurements were 0.895 [95% confidence interval (CI): 0.824–0.936] for C5 root, 0.852 (95% CI: 0.719–0.910) for C6 root, 0.912 (95% CI: 0.801–0.958) for C7 root, and 0.913 (95% CI: 0.822–0.973) for C8 root, respectively. ICCs for inter-observer agreement of SNR value were 0.821 (95% CI: 0.787–0.941) for C5 root, 0.840 (95% CI: 0.713–0.910) for C6 root, 0.802 (95% CI: 0.709–0.848) for C7 root, and 0.814 (95% CI: 0.742–0.853) for C8 root. No differences were found between the right and left nerve root values ($P>0.05$).

The 3D SHINKEI coronal images of brachial plexus of HCs and ALS patients are shown in *Figure 2*. The statistical results are presented in *Figure 3*, *Figure 4*, and *Table 2*. For each point, the diameters at point 1 and point 2 of C6–C8 roots were increased in patients with ALS compared with HCs and the diameters at point 4 and point 5 of C7 roots

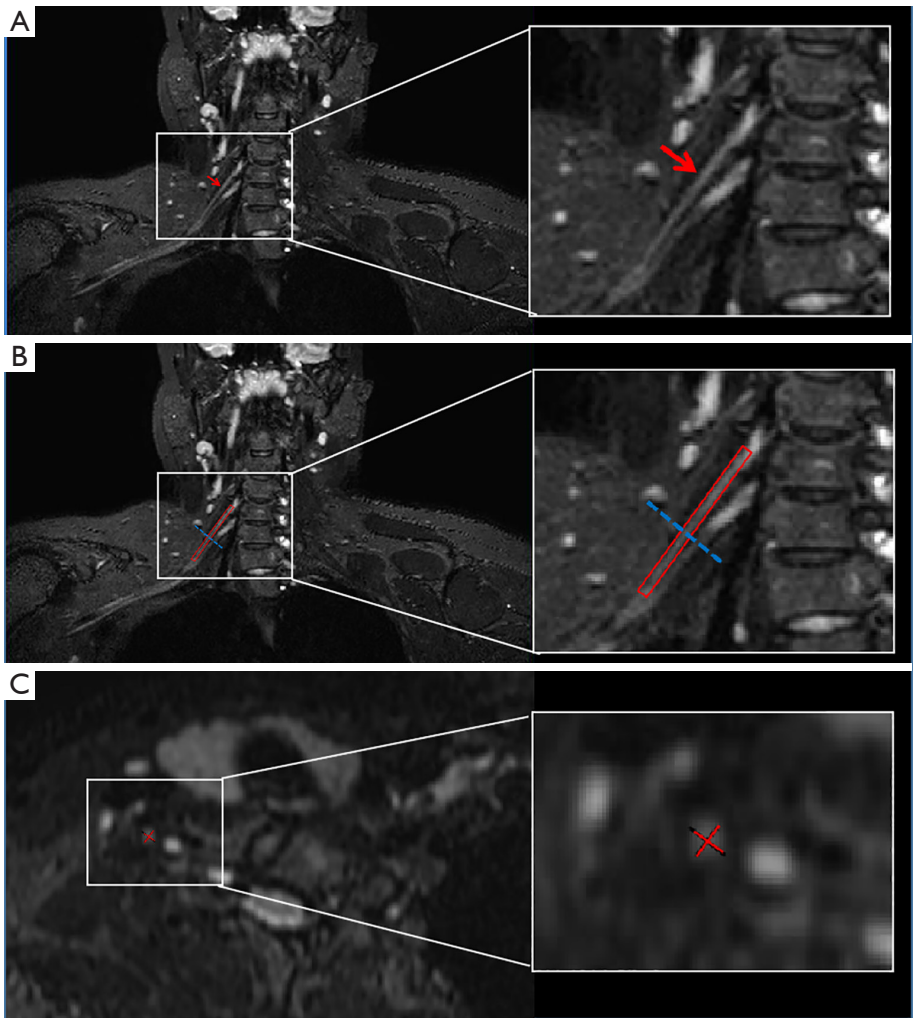

Figure 1 The measurement of diameter. (A) The original image of 3D SHINKEI shows the reconstruction of right C5 root (red arrow). (B) The red rectangle showed the range of right C5 root that was divided into 5 equal segments to identify five points and the dotted line showed the orientation of the axial reformatted of the right C5 root. (C) The corresponding reconstructed image shows the axis of a contour of right C5 root. The red cross shows the measurement of diameter in ROI. The diameter was calculated by the average of the longest diameter and shortest diameter at each ROI. 3D SHINKEI, 3-dimensional nerve-sheath signal increased with inked rest-tissue rapid acquisition of relaxation imaging; ROI, region of interest.

were decreased in patients with ALS compared with HCs. The SNR values at point 5 of C6–C8 roots and point 4 of C7 root were decreased in patients with ALS compared with HCs.

Nerve diameters and SNR values tended towards a statistically significant decrease from proximal to distal except for the SNR value of C5 in HCs. The nerve diameters for ALS patients were more negatively sloped than HCs for all nerve roots ($P<0.001$ for C5, C6, C7, C8). The nerve SNR values for patients with ALS were more negatively sloped than those for HCs in C6 and C8 roots ($P=0.03$ for C6, $P<0.001$ for C8) yet there were no significant statistical differences in C5 and C7 roots. The variation tendency in each gender is presented in Figure S1, Figure S2, and Table S1.

The ROC curves for the diameter and SNR value ratio (cutoff values, sensitivity, specificity, and the AUC) are shown in *Figure 5* and *Table 3*. The AUCs of the C6, C7, and C8 diameter ratios were higher than that of the C5 diameter ratio.

Table 1 Demographic of patients with ALS patients and healthy controls

Demographic or clinical feature	ALS patients	HCs	P value
No. of cases	21	19	
Sex			0.67
Female	8	9	
Male	13	10	
Age at MRI (years)	61.68±7.17	62.16±8.42	0.85
Body weight (kg)	72.41±12.12	67.63±11.88	0.43
Body height (cm)	168.1±7.83	166.1±8.35	0.21
Duration of symptom onset before MRI (month)	20.19±20.04	–	–

The values are presented as number or mean ± SD. ALS, amyotrophic lateral sclerosis; HC, healthy control; MRI, magnetic resonance imaging; SD, standard deviation.

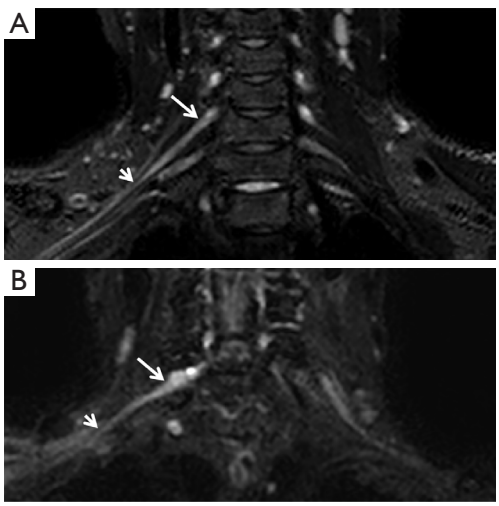

Figure 2 Example 3D SHINKEI images in healthy control participants and ALS patients. (A) The 3D SHINKEI image of right C6 root in healthy control participants shows a slight decrease of diameter from proximal point (long arrows) to distal point (short arrows). (B) The 3D SHINKEI image of right C6 root in ALS patients shows a significant decrease of diameter from proximal point (long arrows) to distal point (short arrows). 3D SHINKEI, 3-dimensional nerve-sheath signal increased with inked rest-tissue rapid acquisition of relaxation imaging; ALS, amyotrophic lateral sclerosis.

Discussion

In this study, the results of 3D MRN imaging reveal that the diameters and SNR values of C5–C8 roots from proximal to distal decreased significantly and in ALS more than HCs. In addition, larger-size diameter changes of the proximal points were observed in C6–C8 roots of the ALS patients. In addition, the distal points demonstrated smaller diameters of C7 roots and smaller SNR values of C5–C8 roots. These results indicated that root alterations were different between proximal and distal points, as suggested in pathophysiological change. The ROC results further revealed the diameter and SNR value ratio of distal point to proximal point could distinguish ALS from HCs with high sensitivity and specificity.

In this study, the proximal nerve enlargement is consistent with the previous report of increased volume in the brachial plexus of ALS patients by Gerevini *et al.* (15). Potential etiologies for these findings could include neuroinflammation, endothelial dysfunction, and nerve edema (16) occurring during the course of ALS. Neuroinflammation is a primary pathologic feature in the ALS pathogenic cascade, characterized by activation and infiltration of monocytes/macrophages surrounding the degenerating peripheral nerve fibers, which occurs even before the onset of clinical signs of motor weakness (17-19). The proximal nerve enlargement might be related to this neuroinflammation and consequent nerve edema and swelling. Interestingly, the results further indicated that the diameters and SNR values of nerve roots at the distal points were decreased compared to controls, which could be a result of reduced myelinated fibers and chronic axonal degeneration (3). Given that ALS is a motor neuronopathy, progressive motor axonal degeneration and nerve fiber loss is considered a major cause of signs and symptoms in ALS (20,21). Furthermore, the changes of nerve diameters and SNR values from proximal to distal are consistent with the pathophysiological changes of ALS in peripheral

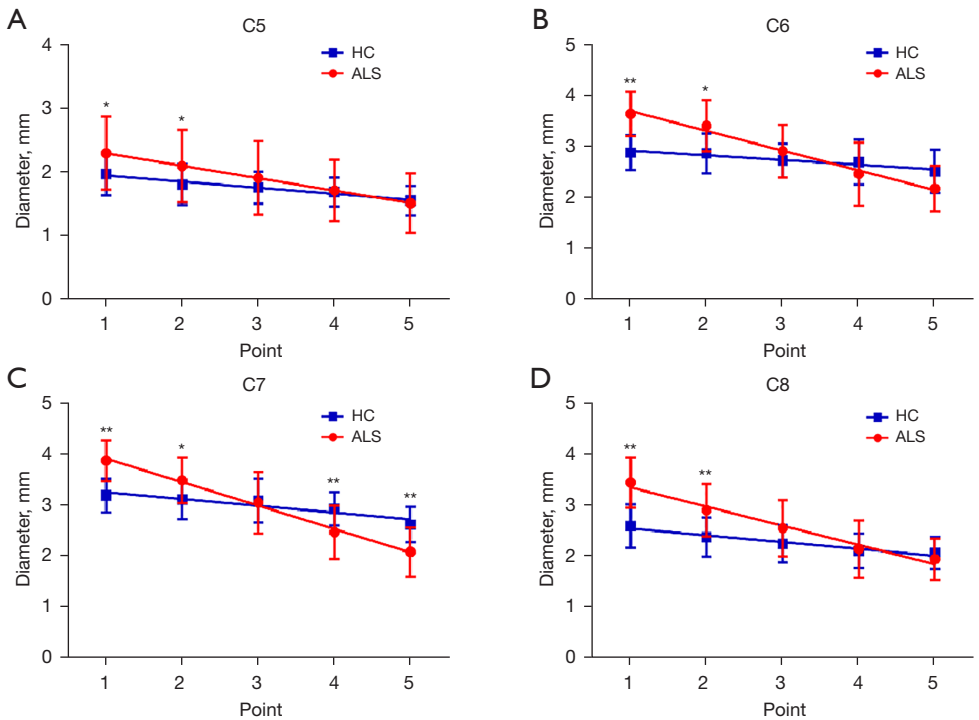

Figure 3 The variation tendency of diameters in C5–C8 (A-D) roots of ALS patients and HCs from proximal to distal location. *, P<0.05 and **, P<0.01 were considered statistically significant. ALS, amyotrophic lateral sclerosis; HC, healthy control.

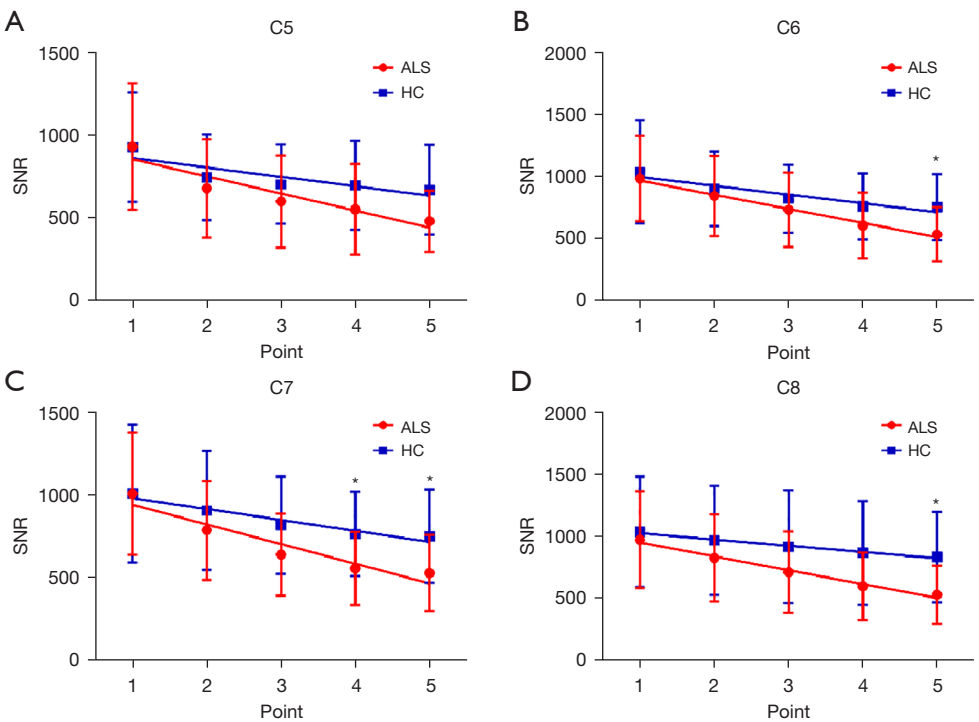

Figure 4 The variation tendency of SNR values in C5–C8 (A-D) roots of ALS patients and HCs from proximal to distal location. *, P<0.05 and were considered statistically significant. ALS, amyotrophic lateral sclerosis; HC, healthy control; SNR, signal-to-noise ratio.

Table 2 The slope values, P values of variation from proximal to distal, and the equation for slope in ALS patients and HCs and differences of slope values between patients with ALS and HCs

Parameter	ALS patients			HCs			P
	Slope value	P value	Equation	Slope value	P value	Equation	
C5 diameter	−0.01924	<0.001*	Y = −0.01924X + 2.500	−0.009422	0.003*	Y = −0.009422X + 2.049	<0.001*
C5 SNR value	−10.14	0.02*	Y = −10.14X + 958.2	−5.552	0.06	Y = −5.552X + 918.5	0.17
C6 diameter	−0.04404	<0.001*	Y = −0.04404X + 4.100	−0.01039	0.01*	Y = −0.01039X + 3.023	<0.001*
C6 SNR value	−12.86	<0.001*	Y = −12.86X + 1081	−8.009	0.01*	Y = −8.009X + 1068	0.03
C7 diameter	−0.06228	<0.001*	Y = −0.06228X + 4.374	−0.01799	0.03*	Y = −0.01799X + 3.382	<0.001*
C7 SNR value	−15.99	0.01*	Y = −15.99X + 1059	−8.900	0.008*	Y = −8.900X + 1046	0.07
C8 diameter	−0.06464	0.001*	Y = −0.06464X + 3.738	−0.02294	0.004*	Y = −0.02294X + 2.684	<0.001*
C8 SNR value	−19.06	<0.001*	Y = −19.06X + 1060	−8.631	<0.001*	Y = −8.631X + 1074	<0.001*

*, P<0.05 was considered statistically significant. ALS, amyotrophic lateral sclerosis; HC, healthy control; SNR, signal-to-noise ratio.

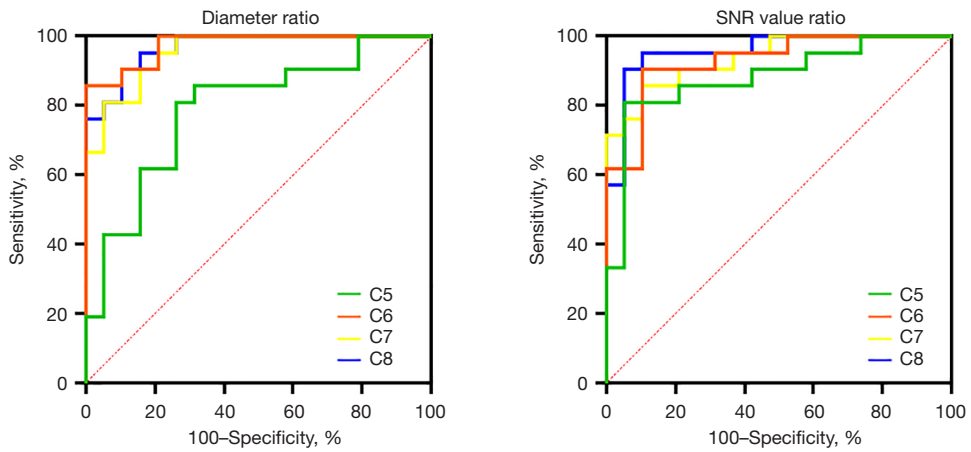

Figure 5 ROC curves for the diameter ratio and SNR value ratio of C5–C8 roots in the diagnosis of ALS. ROC, receiver operating characteristic; SNR, signal-to-noise ratio; ALS, amyotrophic lateral sclerosis.

Table 3 ROC analysis for the diameter ratio and SNR value ratio

Parameter	Sensitivity	Specificity	AUC	Cutoff value
C5 diameter	80.95%	73.68%	0.7895	0.7418
C6 diameter	85.71%	100.00%	0.9749	0.6952
C7 diameter	80.95%	94.74%	0.9549	0.6431
C8 diameter	90.48%	89.47%	0.9674	0.7147
C5 SNR value	80.95%	94.74%	0.8822	0.5989
C6 SNR value	90.48%	89.47%	0.9298	0.6516
C7 SNR value	85.71%	89.47%	0.9373	0.6065
C8 SNR value	90.48%	94.74%	0.9574	0.6758

ROC, receiver operating characteristic; SNR, signal-to-noise; AUC, area under the ROC curve.

nerves, indicating that ALS is a distal axonopathy, a pattern typically seen in peripheral neuropathies with a distal to proximal gradient of damage (4).

The differences from proximal to distal may be related to different disease stages. In this study, one ALS patient imaged 72.3 months after the onset of symptoms demonstrated entire brachial plexus atrophy including the proximal roots, reflecting chronicity of disease process and the late stage of the ALS pathogenetic cascade. This patient was excluded from our study as the markedly atrophic nerve roots were unclear on 3D MRN. Further prospective study with a larger number of patients is needed to ascertain whether this change observed in 3D MRN images is systematically associated with disease course and severity.

There has been contradiction in the literature regarding the diameters of nerve roots of patients with ALS. Most ultrasound studies have suggested that the roots are thinner in patients with ALS (22), whereas increased diameters have been found on the MRI studies (10). This study systematically evaluated the nerve roots at different segments from proximal to distal parts, and found that the signal and size alterations were different, which may account for the controversies above. 3D SHINKEI allowed excellent nerve selective imaging and depiction of the above-described lesions. This also contributed to excellent inter-reader reliability in both signal and size measurements despite the small size of the nerves.

To capture the decrease in nerve root diameters and SNR values from proximal to distal and to facilitate clinical application, the diameter ratio and SNR value ratio of the distal point (point 5) to the proximal point (point 1) in C5–C8 roots was chosen to evaluate the diagnostic performance. The high sensitivity and specificity of the ratio indicated that it may be helpful to evaluate the peripheral neuropathy of ALS. Moreover, the AUCs of C6–C8 diameters were higher than that of C5 diameter, which probably showed that C6–C8 diameters were more sensitive to the assessment of lesions of the peripheral nerves.

This study has some limitations. First, our patient population was small, which was attributed to the rarity of ALS. However, we measured five regions in eight nerve roots (bilateral C5–C8 roots), and the changes from proximal to distal were similar. Second, the diameters of nerve roots were evaluated, not the volumes. However, the diameter was calculated by the average of the longest diameter and shortest diameter at each point, which could produce little effect on the conclusion. In the future, nerve segmentation may help to measure the exact aggregate volumes of the nerves. Third, our study did not account for disease treatment; as there are no detailed studies of disease course and severity, further investigation may be necessary. Fourth, we did not evaluate the entirety of the brachial plexus. Due to its complex form, it is extremely difficult to measure all segments of the brachial plexus. Finally, we did not perform diffusion-weighted or diffusion tensor imaging (DTI). DTI can provide insight into the neuronal architecture. In the future, the DTI evaluation of brachial plexus in patients with ALS using DTI could be explored.

Conclusions

In conclusion, 3D MRN images reveal the proximal-distal longitudinal diameters and SNR values of brachial plexus nerve roots decreased and in ALS more than HCs. These results reflect pathophysiological changes of ALS and may be helpful in improving the diagnosis of ALS. Further prospective study is needed to ascertain whether this change is associated with disease course and severity.

Acknowledgments

Funding: This work was supported by the Natural Science Foundation of Shandong Province (No. ZR2019PH08).

Footnote

Reporting Checklist: The authors have completed the MDAR reporting checklist. Available at https://qims.amegroups.com/article/view/10.21037/qims-23-833/rc

Conflicts of Interest: All authors have completed the ICMJE uniform disclosure form (available at https://qims.amegroups.com/article/view/10.21037/qims-23-833/coif). WC is an employee of Philips Healthcare in Shanghai. The other authors have no conflicts of interest to declare.

Ethical Statement: The authors are accountable for all aspects of the work in ensuring that questions related to the accuracy or integrity of any part of the work are appropriately investigated and resolved. The study was conducted in accordance with the Declaration of Helsinki (as revised in 2013). The study was approved by the institutional ethics committee of Shandong Provincial Hospital and informed consent was provided by all individual participants.

References

1. Turner MR, Swash M. The expanding syndrome of amyotrophic lateral sclerosis: a clinical and molecular odyssey. J Neurol Neurosurg Psychiatry 2015;86:667-73.
2. Saberi S, Stauffer JE, Schulte DJ, Ravits J. Neuropathology of Amyotrophic Lateral Sclerosis and Its Variants. Neurol Clin 2015;33:855-76.
3. Sobue G, Matsuoka Y, Mukai E, Takayanagi T, Sobue I. Pathology of myelinated fibers in cervical and lumbar ventral spinal roots in amyotrophic lateral sclerosis. J Neurol Sci 1981;50:413-21.
4. Fischer LR, Culver DG, Tennant P, Davis AA, Wang M, Castellano-Sanchez A, Khan J, Polak MA, Glass JD. Amyotrophic lateral sclerosis is a distal axonopathy: evidence in mice and man. Exp Neurol 2004;185:232-40.
5. Kronlage M, Bäumer P, Pitarokoili K, Schwarz D, Schwehr V, Godel T, Heiland S, Gold R, Bendszus M, Yoon MS. Large coverage MR neurography in CIDP: diagnostic accuracy and electrophysiological correlation. J Neurol 2017;264:1434-43.
6. Fortanier E, Ogier AC, Delmont E, Lefebvre MN, Viout P, Guye M, Bendahan D, Attarian S. Quantitative assessment of sciatic nerve changes in Charcot-Marie-Tooth type 1A patients using magnetic resonance neurography. Eur J Neurol 2020;27:1382-9.
7. Wu F, Wang W, Yang Y, Li C, Wu J, Liu H, Ren Y. MR neurography of lumbosacral nerve roots for differentiating chronic inflammatory demyelinating polyneuropathy from acquired axonal polyneuropathies: a cross-sectional study. Quant Imaging Med Surg 2022;12:4875-84.
8. Kronlage M, Knop KC, Schwarz D, Godel T, Heiland S, Bendszus M, Bäumer P. Amyotrophic Lateral Sclerosis versus Multifocal Motor Neuropathy: Utility of MR Neurography. Radiology 2019;292:149-56.
9. Rajabally YA, Jacob S. Chronic inflammatory demyelinating polyneuropathy-like disorder associated with amyotrophic lateral sclerosis. Muscle Nerve 2008;38:855-60.
10. Staff NP, Amrami KK, Howe BM. Magnetic resonance imaging abnormalities of peripheral nerve and muscle are common in amyotrophic lateral sclerosis and share features with multifocal motor neuropathy. Muscle Nerve 2015;52:137-9.
11. Kasper JM, Wadhwa V, Scott KM, Rozen S, Xi Y, Chhabra A. SHINKEI--a novel 3D isotropic MR neurography technique: technical advantages over 3DIRTSE-based imaging. Eur Radiol 2015;25:1672-7.
12. Yoneyama M, Takahara T, Kwee TC, Nakamura M, Tabuchi T. Rapid high resolution MR neurography with a diffusion-weighted pre-pulse. Magn Reson Med Sci 2013;12:111-9.
13. Brooks BR, Miller RG, Swash M, Munsat TL; World Federation of Neurology Research Group on Motor Neuron Diseases. El Escorial revisited: revised criteria for the diagnosis of amyotrophic lateral sclerosis. Amyotroph Lateral Scler Other Motor Neuron Disord 2000;1:293-9.
14. Kundel HL, Polansky M. Measurement of observer agreement. Radiology 2003;228:303-8.
15. Gerevini S, Agosta F, Riva N, Spinelli EG, Pagani E, Caliendo G, Chaabane L, Copetti M, Quattrini A, Comi G, Falini A, Filippi M. MR Imaging of Brachial Plexus and Limb-Girdle Muscles in Patients with Amyotrophic Lateral Sclerosis. Radiology 2016;279:553-61.
16. Stoll G, Müller HW. Nerve injury, axonal degeneration and neural regeneration: basic insights. Brain Pathol 1999;9:313-25.
17. Evans MC, Couch Y, Sibson N, Turner MR. Inflammation and neurovascular changes in amyotrophic lateral sclerosis. Mol Cell Neurosci 2013;53:34-41.
18. Philips T, Robberecht W. Neuroinflammation in amyotrophic lateral sclerosis: role of glial activation in motor neuron disease. Lancet Neurol 2011;10:253-63.
19. Schreiber S, Schreiber F, Garz C, Debska-Vielhaber G, Assmann A, Perosa V, Petri S, Dengler R, Nestor P, Vielhaber S. Toward in vivo determination of peripheral nervous system immune activity in amyotrophic lateral sclerosis. Muscle Nerve 2019;59:567-76.
20. Riva N, Chaabane L, Peviani M, Ungaro D, Domi T, Dina G, Bianchi F, Spano G, Cerri F, Podini P, Corbo M, Carro UD, Comi G, Bendotti C, Quattrini A. Defining peripheral nervous system dysfunction in the SOD-1G93A transgenic rat model of amyotrophic lateral sclerosis. J Neuropathol Exp Neurol 2014;73:658-70.
21. Devigili G, Uçeyler N, Beck M, Reiners K, Stoll G,

Toyka KV, Sommer C. Vasculitis-like neuropathy in amyotrophic lateral sclerosis unresponsive to treatment. Acta Neuropathol 2011;122:343-52.
22. Mori A, Nodera H, Takamatsu N, Maruyama-Saladini K, Osaki Y, Shimatani Y, Oda M, Izumi Y, Kaji R. Sonographic evaluation of cervical nerve roots in ALS and its clinical subtypes. J Med Invest 2016;63:54-7.

Cite this article as: Wang S, Man X, Chen Y, Gong T, Gao F, Chen W, Wang G, Zhao B, Chhabra A. Three-dimensional magnetic resonance neurography aids in detection of brachial plexus nerve root signal and size alterations in patients with amyotrophic lateral sclerosis: a case-control study. Quant Imaging Med Surg 2023;13(12):8694-8703. doi: 10.21037/qims-23-833

Supplementary

Table S1 The P values of diameter and SNR value variation from proximal to distal for females and males and differences of slope values between patients with ALS and HCs

Parameter	P values of variation in ALS Patients		P values of variation in HCs		The difference of slope values	
	Females	Males	Females	Males	Females	Males
C5 diameter	P<0.001*	P<0.001*	P=0.02*	P<0.001*	P=0.002*	P<0.001*
C5 SNR value	P=0.02*	P=0.02*	P=0.18	P=0.02*	P=0.12	P=0.25
C6 diameter	P<0.001*	P<0.001*	P=0.02*	P=0.02*	P<0.001*	P<0.001*
C6 SNR value	P<0.001*	P<0.001*	P=0.02*	P=0.01*	P=0.01*	P=0.11
C7 diameter	P<0.001*	P<0.001*	P=0.08	P=0.004*	P=0.007*	P<0.001*
C7 SNR value	P=0.009*	P=0.017*	P=0.017*	P=0.004*	P=0.012*	P=0.24
C8 diameter	P=0.003*	P=0.007*	P=0.016*	P=0.002*	P=0.002*	P<0.001*
C8 SNR value	P=0.003*	P=0.004*	P=0.002*	P=0.004*	P=0.002*	P=0.002*

*, P<0.05 was considered statistically significant.

https://dx.doi.org/10.21037/qims-23-833

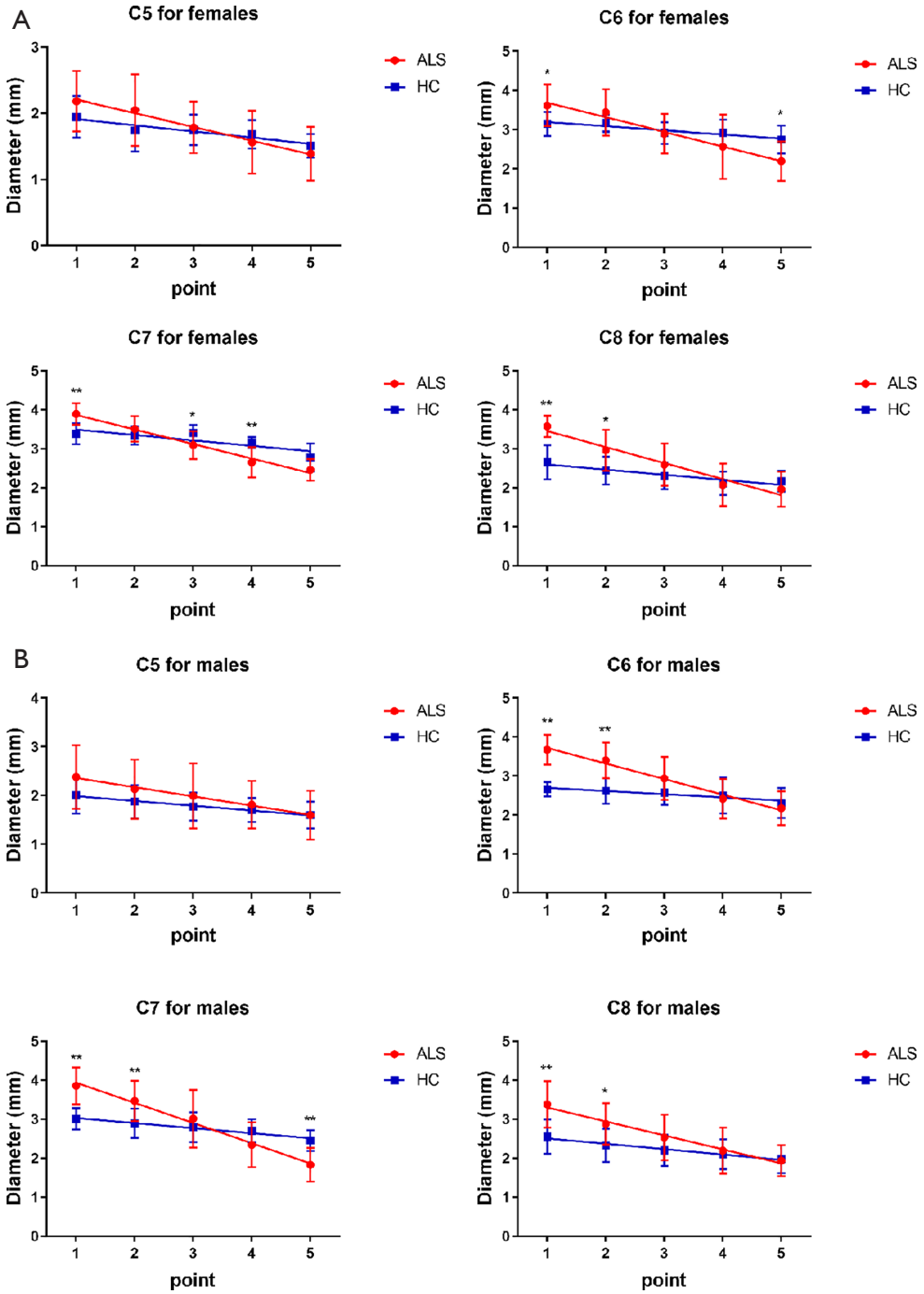

Figure S1 The variation tendency of C5–C8 diameters of ALS patients and HCs from proximal to distal location in the females (A) and males (B). *, P<0.05 and **, P<0.01 were considered statistically significant.

https://dx.doi.org/10.21037/qims-23-833

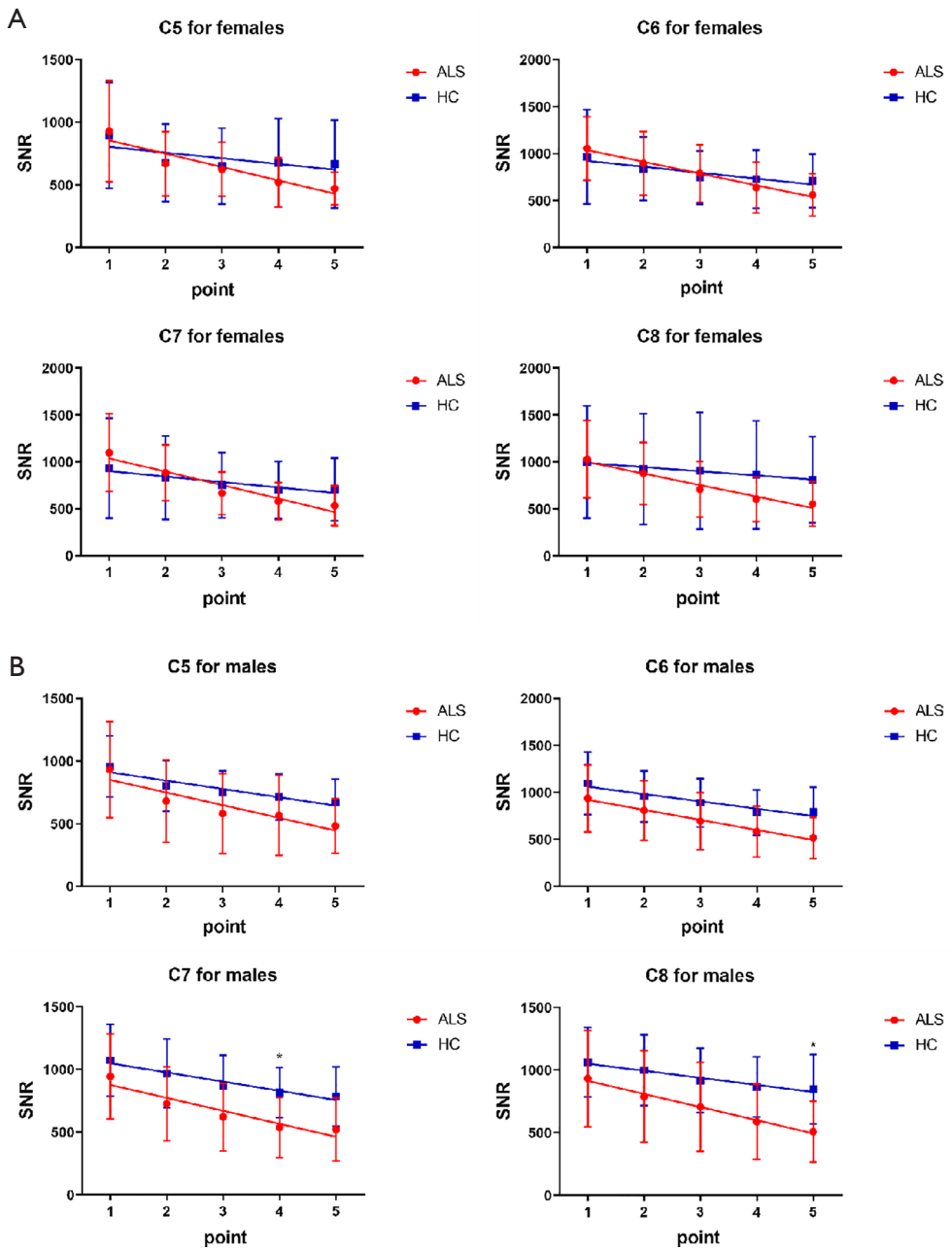

Figure S2 The variation tendency of SNR values of ALS patients and HCs from proximal to distal location in the females (A) and males (B). *, P<0.05 and **, P<0.01 were considered statistically significant.

https://dx.doi.org/10.21037/qims-23-833